2.B

Nuclear Physics A117 (1968) 343—352; © *North-Holland Publishing Co., Amsterdam*

^{6}Li(p, ^{3}He)^{4}He REACTION WITH POLARIZED PROTONS FROM 0.4 TO 3.2 MeV

LOUIS BROWN

Department of Terrestrial Magnetism, Carnegie Institution of Washington †, *Washington, D.C.*

and

CLAUDE PETITJEAN ††

Department of Physics, University of Basel, Switzerland

Received 10 June 1968

Abstract: A polarized beam was used to measure the asymmetry in the angular distribution of the particles from the ^{6}Li(p, ^{3}He)^{4}He reaction at 15 different energies from 0.4 to 3.2 MeV. The polarization efficiency can be fitted with associated Legendre polynomials. At 1 MeV and below the coefficient of P_1^1 is large and all other terms are negligible. Above 1 MeV, the coefficients of P_2^1 and P_3^1 are also significant. The data were measured typically to an accuracy of 2 % with a target 30 keV thick at 1 MeV bombarding energy. A polarization contour map is given. The polarization is generally large and positive.

E NUCLEAR REACTION ^{6}Li(polarized p, ^{3}He), E = 0.4–3.2 MeV; measured polarization analysing power. Enriched target.

1. Introduction

The first comprehensive study of the reaction ^{6}Li(p, ^{3}He)^{4}He was made in 1938 by Rumbaugh, Roberts and Hafstad [1]) using separated isotopes in experiments that measured the energy dependence of the relative yields of seven reactions involving ^{6}Li and ^{7}Li. Since then the interaction has been measured repeatedly [2–9]) in the energy range below 3 MeV, and the intermediate nucleus ^{7}Be has also been studied with ^{6}Li(p, p)^{6}Li by a smaller number of investigators [3,10–12]), with ^{4}He(^{3}He, ^{3}He)^{4}He by Tombrello *et al.* [13–14]) and with ^{6}Li(p, γ)^{7}Be in two other experiments [15–16]). These experiments were not sensitive to polarization effects and have not established beyond dispute the structure of ^{7}Be, shown on the basis of present knowledge in fig. 1. All experiments disclose a $\frac{5}{2}^{-}$ p-state at 1.87 MeV proton energy (7.21 MeV excitation energy); 500 keV below is another $\frac{5}{2}^{-}$ state that is revealed in ^{3}He–^{4}He scattering but is not observed with incident protons, probably because it is an f-state. Recently Bouchez *et al.* [5–8]) measured angular distributions of ^{6}Li(p, ^{3}He)^{4}He at low energies, which they could reproduce by introducing a $\frac{3}{2}^{-}$ state at 0.35 MeV and a $\frac{3}{2}^{+}$

† Experiment performed at the Carnegie Institution of Washington.

†† Fellow of the Swiss National Foundation and the Carnegie Institution of Washington.

state at 0.70 MeV into the structure. Neither of these states is observed in p-^{6}Li scattering [10]), ^{3}He-^{4}He scattering [13-14]) or proton capture [16]). Mani and Dix [17]) report a level of unknown spin and parity in ^{7}Li by observing protons scattered inelastically from it, a level not seen in α-^{3}H-scattering [14]), a corresponding level in the mirror nucleus ^{7}Be would lie near the levels that Bouchez proposes.

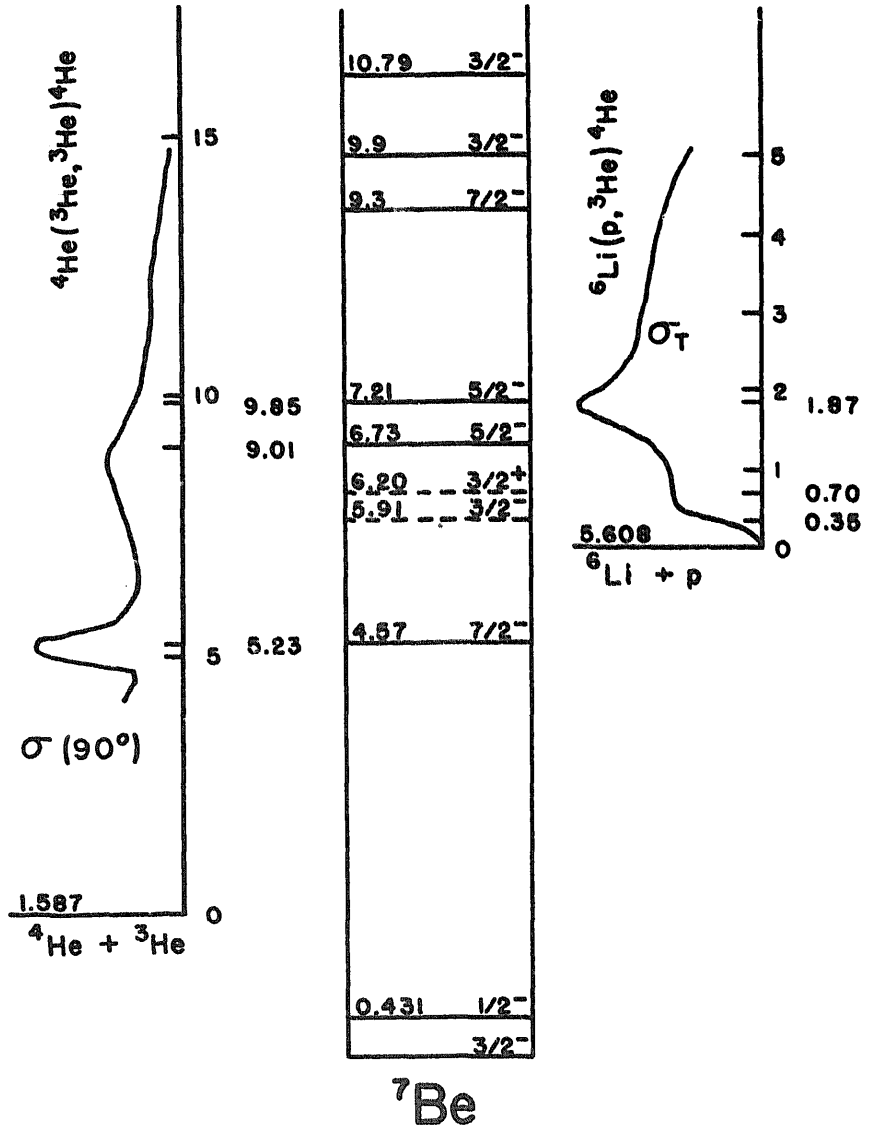

Fig. 1. Energy level diagram of the nucleus ^{7}Be. The portion of the structure that is accessible to experiment by bombarding ^{6}Li with protons is indicated at the right with the total reaction cross section plotted as a function of proton lab energy. A similar diagram for ^{3}He on ^{4}He is shown at the left with the differential cross section at $\theta_{c.m.} = 90°$ plotted as a function of ^{3}He lab energy. The two levels represented by dashed lines have been proposed by Bouchez *et al.* [5-8]).

We have studied the behaviour of the ^{6}Li(p, ^{3}He)^{4}He reaction with an incident beam of polarized protons and find a large polarization efficiency, which we measured in sufficient detail to be useful in an analysis of the structure of ^{7}Be. Of practical

value is the discovery that this reaction has large polarization efficiency at low energies. Experimentalists constructing sources of polarized protons have had to content themselves with reactions that are efficient polarization analysers at energies above 1 MeV, the favorites are ^{4}He(p, p)^{4}He and ^{12}C(p, p)^{12}C. These are inconvenient for testing some sources, and recourse is generally taken to the ^{3}H(d, n)^{4}He and ^{3}He (d, p)^{4}He reactions. These two give very useful information about the operation of sources but are not tests of them for protons and are, of course, of no use whatsoever to someone who might care to examine the polarization of low-energy protons from reactions. The ^{6}Li(p, ^{3}He) ^{4}He reaction fills these needs splendidly. It has polarization efficiency of 0.6 at 1 MeV, a smooth variation with energy and scattering angle, a Q-value of 4.02 MeV, which makes identification of the reaction products easy at low proton energy, and a total cross section of about 100 mb, which is sufficiently large for rapid determination of the polarization for the beams of most sources.

2. Experimental technique

The apparatus for this experiment is the same as that used in work [18]) on ^{7}Li(p, α) ^{4}He with two exceptions: the ^{6}Li is evaporated onto a 50 nm nickel foil in a chamber that is part of the vacuum system of the target chamber rather than external to it, and the reaction products are observed with surface barrier detectors rather than scintillation detectors.

The lithium, enriched to 99.3 % ^{6}Li, was first heated under high vacuum near a liquid nitrogen trap and with the target backing in another compartment of the vacuum system. When the hydrocarbons were driven off, the lithium was evaporated onto the foils during a period of about 1 h, after which time the targets were transferred in vacuum to the target chamber. The preparation technique was sufficiently reproducible that all targets were, within 5 keV error limits, 30 keV thick at 1 MeV. The target thickness was measured by observing the shift in energy needed to excite the 874 keV resonance of the ^{19}F(p, $\alpha\gamma$)^{16}O reaction when the target is inserted into the beam.

This target allowed us, depending on the energy and angle, to resolve the charged particle groups in the detector spectra: the reaction products ^{3}He and ^{4}He and the protons elastically scattered by nickel, lithium and the target impurities oxygen, nitrogen, carbon and hydrogen. The impurities, which, except for hydrogen, could not be resolved one from the other, increased with the age of the target. Fresh targets were made when the impurities interfered with the resolution. At low energies, the large Rutherford cross section of nickel made it difficult to measure in the forward direction; the information could be obtained, however, from the recoiling ^{4}He seen at backward angles. At high energies, the reaction products have energies that cause them to be confused at backward angles with elastically scattered protons; the information could be obtained from the recoiling ^{4}He seen at forward angles. A sample of a detector spectrum is shown in fig. 2.

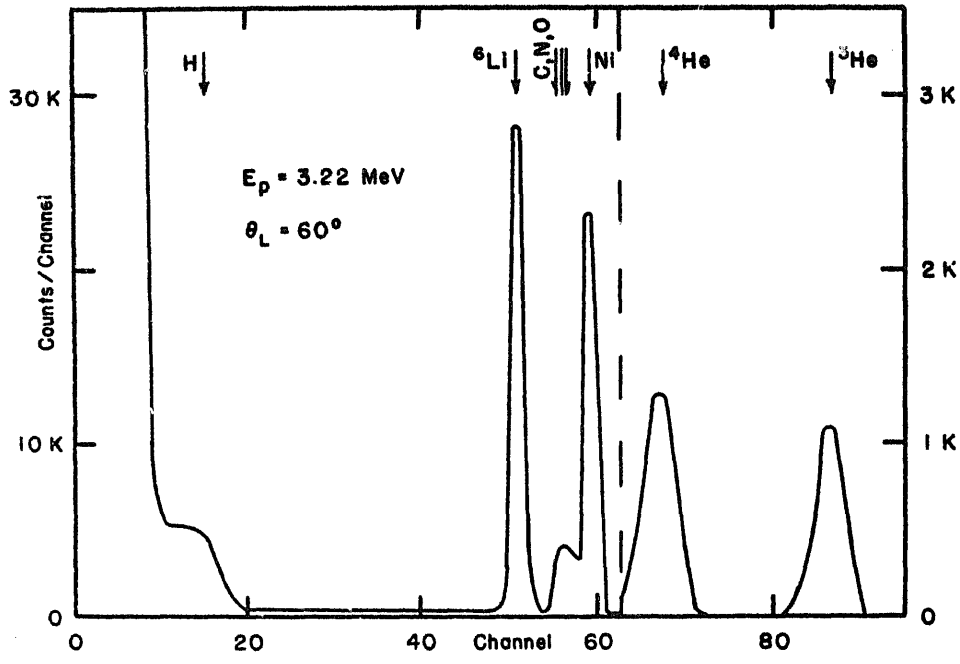

Fig. 2. An example of the spectrum from one of the charged particle detectors. The counts per channel, which resulted from 10 min of data accumulation, have been connected with a smooth curve. The portion to the left of the vertical dashed line has the scale of the left margin; the portion to the right has that of the right margin. The right-hand portion shows the two particle groups from the reaction and the left-hand portion the protons elastically scattered by the nickel target backing, the lithium and the target contaminants; the energies of the reaction products and the elastically scattered protons are indicated with small vertical arrows at the top of the drawing, the positions of which are calculated relative to the ^{3}He line. The two detectors were almost identical in noise and resolution.

3. Results

The differential cross section for unpolarized protons can be written

$$\sigma_0(E,\theta) = \frac{\sigma_{\text{tot}}}{4\pi}\,[1+B_1(E)P_1(\cos\theta)+B_2(E)P_2(\cos\theta)+\ldots], \tag{1}$$

where θ is the reaction angle, B_i the energy dependent coefficients and σ_{tot} the total reaction cross section. If the incident protons are polarized, the expression has to be enlarged to [19])

$$\sigma_p(E,\theta,\phi) = \sigma_0(E,\theta)[1+P_b P_a(E,\theta)\cos\phi], \tag{2}$$

where P_b is the incident proton polarization perpendicular to the direction of the beam, ϕ the azimuthal angle between the normal to the reaction plane defined according to the Basel sign convention and the axis of polarization and P_a the analysing efficiency of the reaction, which can be written

$$P_a = \frac{A_1(E)P_1^1(\cos\theta)+A_2(E)P_2^1(\cos\theta)+\ldots}{1+B_1(E)P_1(\cos\theta)+B_2(E)P_2(\cos\theta)+\ldots}. \tag{3}$$

The Legendre functions are defined by Jahnke and Emde [20]).

Fig. 3 shows the measured datum points and curves fitted to them with eq. (3) using the procedure of least-squares. A table of the numerical values of the data has been deposited with the National Auxiliary Publications Service †. The values of the coefficients B_i were obtained by averaging the values of refs. [4,8,9]) with smooth curves. Table 1 gives the values of the A_i determined by this experiment, the values of the B_i used in the calculations and the quality of fit ε^2 defined as

$$\varepsilon^2 = \frac{1}{n-m}\sum_{j=1}^{n}\left[\frac{P_{\text{meas}}(\theta_j)-P_{\text{cal}}(\theta_j)}{\Delta P_j}\right]^2, \tag{4}$$

where n is the number of datum points, m the number of associated Legendre functions used in the fit, P_{meas} the measured polarization efficiency, ΔP_j the experimental error and P_{cal} the value obtained by substituting the tabulated coefficients in eq. 3.

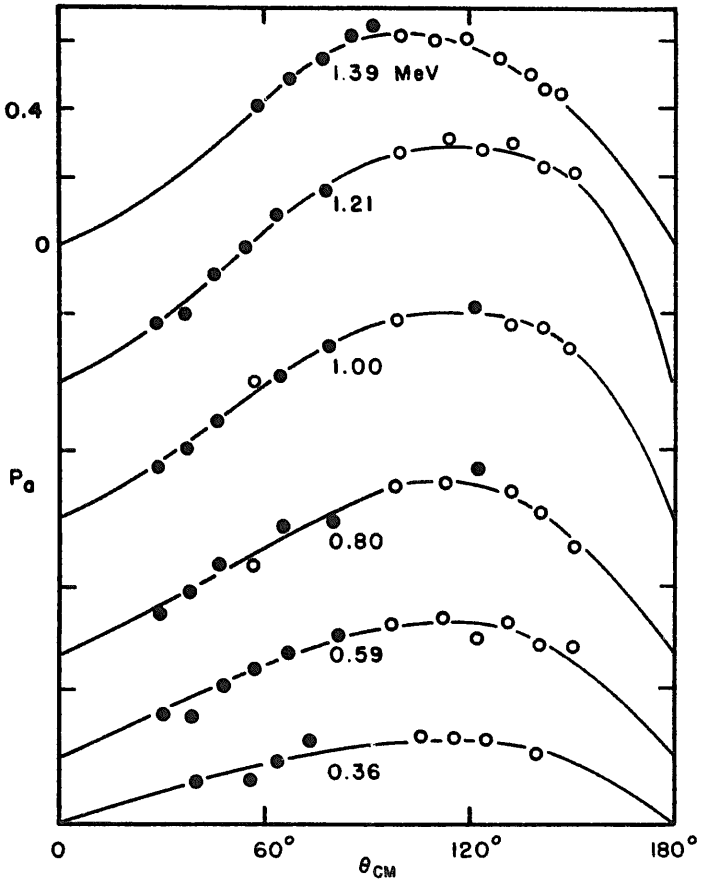

Fig. 3a. Angular distributions of the polarization efficiency of ^{6}Li(p,^{3}He)^{4}He plotted as functions of center-of-mass scattering angle. The vertical scale is the same for all drawings and can be ascertained at the upper left margin of each drawing. The open circles show points measured from observations of the ^{3}He and the closed circles the points obtained from observations of the recoil ^{4}He. The radius of the circles is approximately the experimental error. The smooth curves are calculated with eq. (3) using the coefficients listed in table 1.

† For a copy of this table, order Document NAPS-00067 from the National Auxiliary Publications Service of the American Society for Information Sciences, c/o CCM Information Sciences, Inc., 22 West 34th Street, New York, N.Y. 10001, remitting $ 1.00 for microfiche or $ 3.00 for photocopies.

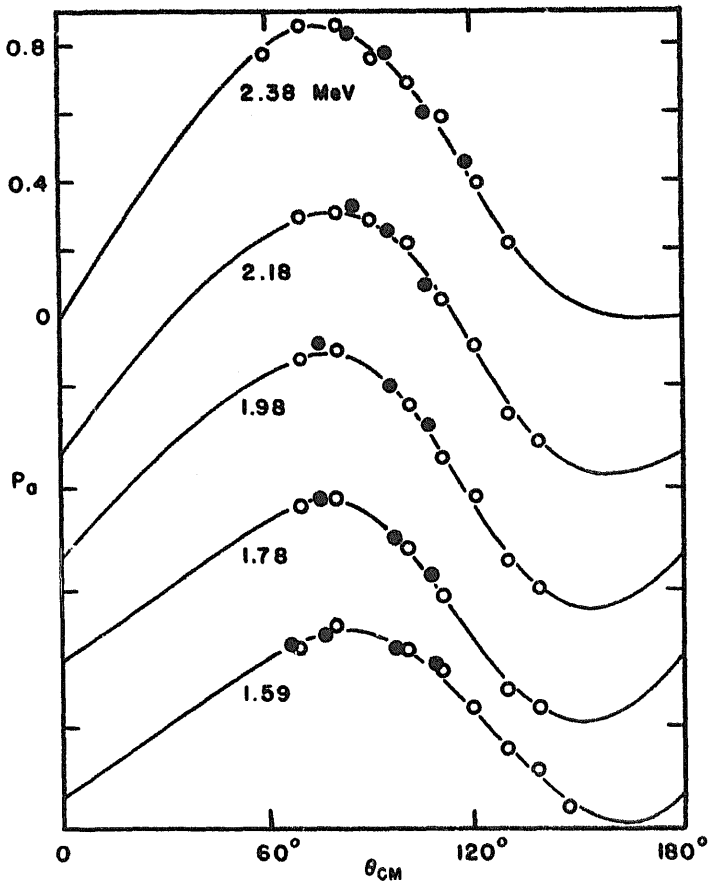

Fig. 3b. For caption see fig. 3a.

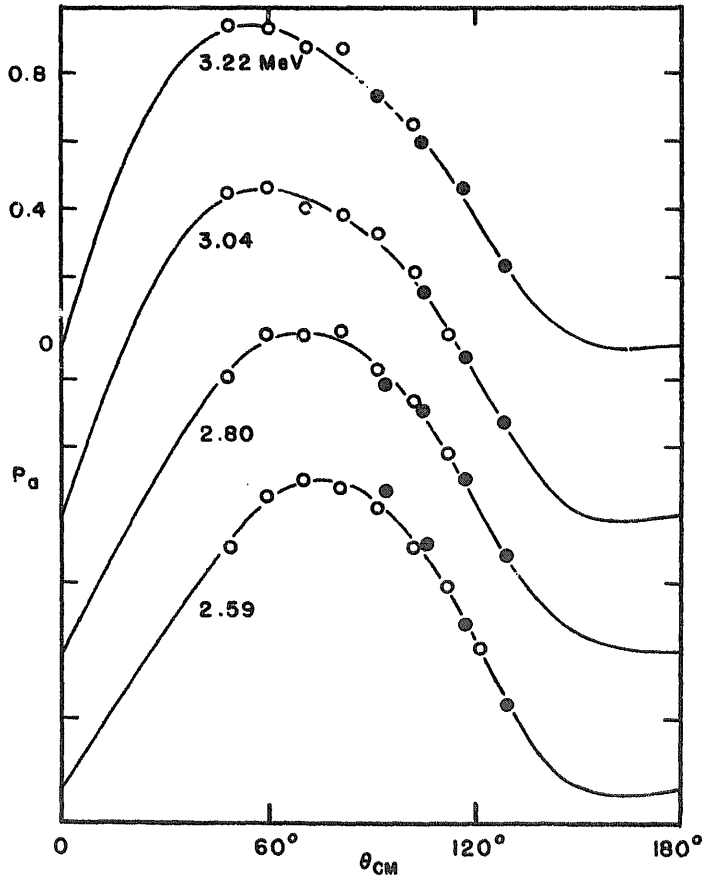

Fig. 3c. For caption see fig. 3a.

TABLE 1

Coefficients of the Legendre functions as used in eq. (3) that give the best fit to the experimental results

Energy (MeV)	B_1	B_2	B_3	B_4	A_1	ΔA_1	A_2	ΔA_2	A_3	ΔA_3	A_4	ΔA_4	ε^2
0.36	0.27	−0.13			0.247	0.012	−0.005	0.007					0.82
0.59	0.40	−0.015			0.368	0.009	0.001	0.007					1.43
0.80	0.49	0.0			0.450	0.011	0.005	0.007	−0.009	0.005	0.000	0.005	2.00
1.00	0.57	−0.02			0.545	0.007	0.019	0.004	−0.013	0.003	−0.010	0.003	0.75
1.21	0.63	−0.11			0.623	0.008	0.029	0.005	−0.032	0.004	−0.010	0.004	1.21
1.39	0.67	−0.13			0.575	0.005	0.058	0.002	−0.048	0.002	−0.009	0.002	0.69
1.59	0.67	0.01			0.423	0.005	0.137	0.003	−0.031	0.003	−0.004	0.002	0.73
1.78	0.50	0.23			0.320	0.004	0.176	0.004	−0.034	0.003	−0.002	0.002	0.62
1.98	0.13	0.29			0.416	0.007	0.180	0.006	−0.044	0.004	0.020	0.004	1.43
2.18	0.10	0.30	−0.08	0.02	0.551	0.006	0.171	0.006	−0.031	0.004	0.017	0.004	1.05
2.38	0.11	0.28	−0.06	0.07	0.683	0.007	0.189	0.006	−0.019	0.005	0.007	0.005	1.46
2.59	0.10	0.22	−0.075	0.10	0.734	0.008	0.197	0.004	−0.044	0.007	0.006	0.004	1.78
2.80	0.07	0.15	−0.11	0.10	0.786	0.007	0.215	0.004	−0.029	0.006	0.000	0.004	0.83
3.04	0.05	0.08	−0.18	0.095	0.807	0.008	0.267	0.005	−0.009	0.006	0.014	0.005	1.10
3.22	0.05	0.00	−0.22	0.085	0.785	0.010	0.272	0.004	−0.005	0.008	0.006	0.006	1.08

For each value of the mean reaction energy given in MeV in the first column is listed the coefficients B_i obtained by averaging the values of refs. [4,8,9]) with smooth curves, the best fit values of the A_i with their uncertainties and the quality of fit ε^2 defined by eq. (4).

Fig. 4 shows plots of A_1, A_2 and A_3 as functions of energy. The values of the coefficients at given energies have been connected by smooth curves fitted by eye; from these curves the curve of the polarization analysing efficiency for lab angle 90° shown with measurements in the upper half of fig. 4 was calculated. The data were taken at fixed angle for several values of energy, so that all of the angular distributions have points taken at times separated by several days or weeks. This gave a continual check on the polarization of the beam during the course of the experiment, since points taken at the same energy with beams of different polarization would show

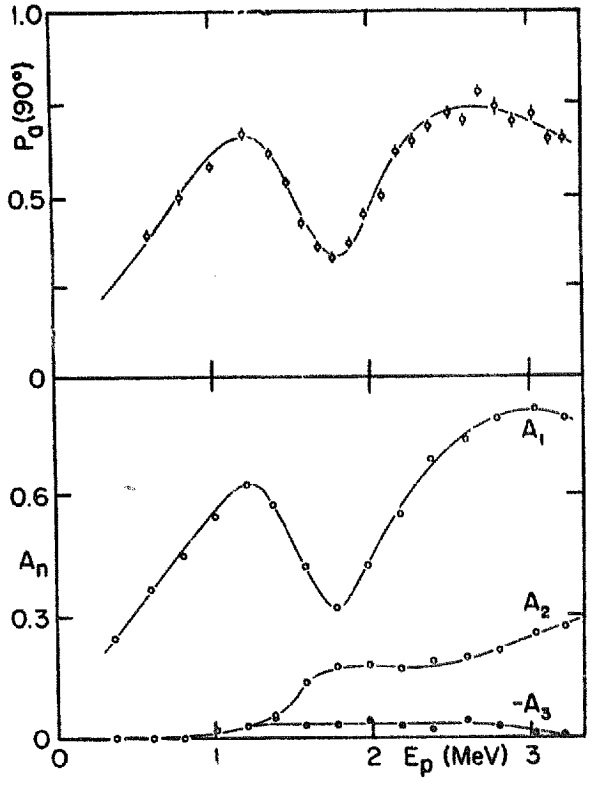

Fig. 4. Polarization excitation function at lab angle 90° and the coefficients A_1, A_2 and A_3 plotted as functions of proton lab energy. The points plotted for the A_i are those of table 1, which have been connected with smooth curves fitted by eye. From these curves, the curve of the polarization efficiency for lab angle 90° shown in the upper diagram was calculated. Measurements at 90° were taken at additional energies to those of the angular distributions.

systematic deviations in the fits with eq. (3). No such deviations were noted. The coefficients B_i were varied within the limits allowed by the original unpolarized data to see if better fits could be obtained; the polarization is not particularly sensitive to them, however, and we saw no reason to alter the values extracted from the unpolarized measurements. We could not find an anomaly in A_2 similar to the behaviour of B_2, on which Bouchez *et al.* [8]) base the 0.35 MeV state.

4. Conclusions

The only structure evident from the plots of the coefficients A_i as functions of energy is the undisputed resonance at 1.87 MeV, which appears in A_1 and A_2. The large value and rapid rise from zero energy of A_1, which indicates s- and p-wave interference is surprising, and it is not clear whether it can be explained with a multi-level analysis or by direct interaction.

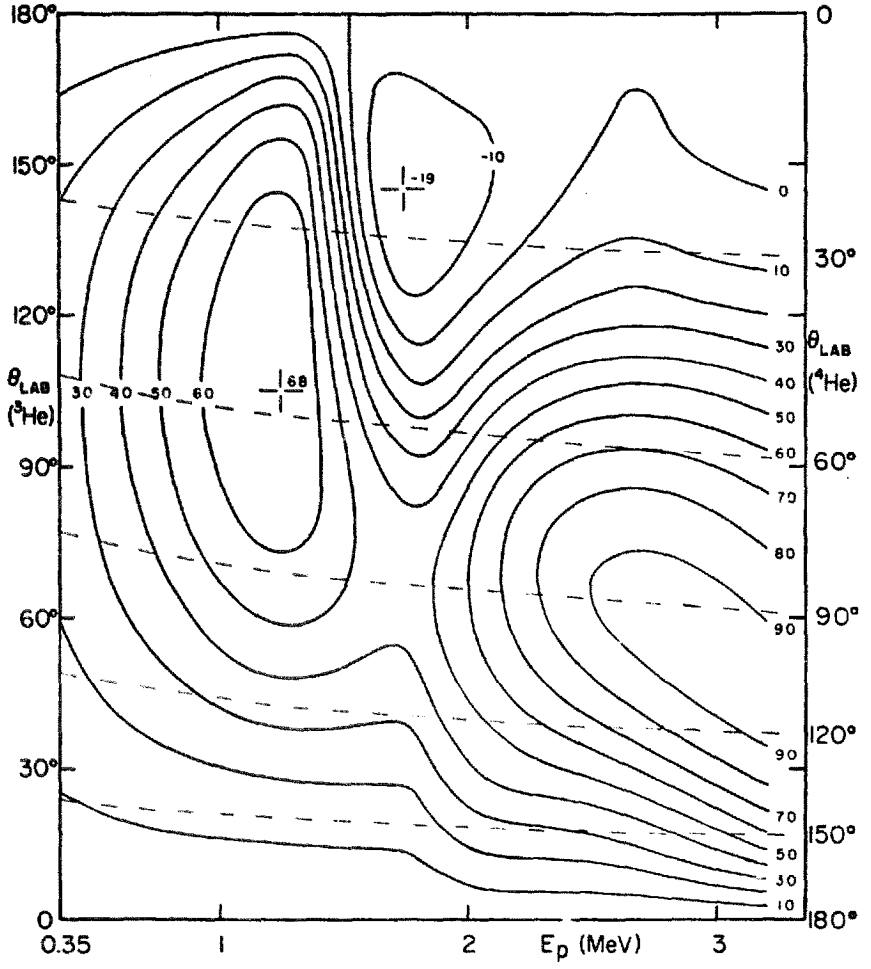

Fig. 5. Polarization contour map of the reaction ^{6}Li(p, ^{3}He)^{4}He. Analysing efficiency contours of 0.1 spacing, which are calculated from the smooth curves of the A_i in fig. 4, are shown plotted on a rectangular coordinate system of lab reaction angle against lab proton energy. The recoil ^{4}He is equally useful for analysing proton polarization so we have added curved grid lines to show the lab angles of the α-particles; the angles in the left margin are for the ^{3}He coordinate system and those in the right margin for the ^{4}He coordinate system, which has dashed lines to indicate every 30°. When used for ^{4}He as the outgoing particle, the sign of the polarization efficiency must be reversed.

Fig. 5 is a polarization contour map of the reaction, which is included to simplify its use as an analyser of polarized protons. Analysing efficiency contours of 0.1 spacing, which are calculated from the smooth curves of the A_i in fig. 4, are shown

plotted on a rectangular coordinate system of lab reaction angle against lab proton energy. The recoil ^{4}He is equally useful for analysing proton polarization, so we have added curved grid lines to show the lab angles of the α-particles; the angles in the left margin are for the ^{3}He coordinate system and those in the right margin for the ^{4}He coordinate system, which has dashed lines to indicate every 30°. When used for ^{4}He as the outgoing particle, the sign of the polarization efficiency must be reversed.

References

1) L. H. Rumbaugh, R. B. Roberts and L. R. Hafstad, Phys. Rev. **54** (1938) 657
2) W. E. Burcham and J. M. Freeman, Phil. Mag. **41** (1950) 921
3) S. Bashkin and H. T. Richards, Phys. Rev. **84** (1951) 1124
4) J. B. Marion, G. Weber and F. S. Mozer, Phys. Rev. **104** (1956) 1402
5) R. Bouchez, C. Delorme, J. Fleury, J. Krafft, P. Perrin, L. Goldman, M. Boge and B. Dudek, J. de Phys. **21** (1960) 346
6) N'Guyen Huu Khanh, L. Goldman and R. Bouchez, J. de Phys. **22** (1961) 267
7) H. Beaumevielle, N. Longequeue and J. P. Longequeue, Compt. Rend. **256** (1963) 1494
8) H. Beaumevielle, J. P. Longequeue, N. Longequeue and R. Bouchez, J. de Phys. **25** (1964) 933
9) J. M. F. Jeronymo, G. S. Mani and A. Sadeghi, Nucl. Phys. **43** (1963) 424
10) J. A. McCray, Phys. Rev. **130** (1963) 2034
11) W. D. Harrison and A. B. Whitehead, Phys. Rev. **132** (1963) 2607
12) U. Fasoli, E. A. Silverstein, D. Toniolo and G. Zago, Nuovo Cim. **34** (1964) 1832
13) T. A. Tombrello and P. D. Parker, Phys. Rev. **130** (1963) 1112
14) R. J. Spiger and T. A. Tombrello, Phys. Rev. **163** (1967) 964
15) S. Bashkin and R. R. Carlson, Phys. Rev. **97** (1955) 1245
16) J. B. Warren, T. K. Alexander and G. B. Chadwick, Phys. Rev. **101** (1956) 242
17) G. S. Mani and A. D. B. Dix, Nucl. Phys. **A106** (1967) 251
18) C. Petitjean and L. Brown, Nucl. Phys. **A111** (1968) 177
19) L. Wolfenstein, Phys. Rev. **75** (1949) 1664
20) E. Jahnke and F. Emde, Tables of functions (Dover Publications, New York, 1945)